

UC Irvine

UC Irvine Previously Published Works

Title

Disorder-driven non-Fermi-liquid behavior in CeRhRuSi₂

Permalink

<https://escholarship.org/uc/item/7x92r1jq>

Journal

Physical Review B, 61(1)

ISSN

2469-9950

Authors

Liu, Chia-Ying
MacLaughlin, DE
Neto, AH Castro
[et al.](#)

Publication Date

2000

DOI

10.1103/physrevb.61.432

Copyright Information

This work is made available under the terms of a Creative Commons Attribution License, available at <https://creativecommons.org/licenses/by/4.0/>

Peer reviewed

Disorder-driven non-Fermi-liquid behavior in CeRhRuSi₂

Chia-Ying Liu, D. E. MacLaughlin, and A. H. Castro Neto
Department of Physics, University of California, Riverside, California 92521

H. G. Lukefahr
Whittier College, Whittier, California 90608

J. D. Thompson, J. L. Sarrao, and Z. Fisk
Los Alamos National Laboratory, Los Alamos, New Mexico 87545

(Submitted June 3, 1999; revised version submitted September 14, 1999)

We report measurements of the bulk magnetic susceptibility and ²⁹Si nuclear magnetic resonance (NMR) linewidth in the heavy-fermion alloy CeRhRuSi₂. The linewidth increases rapidly with decreasing temperature and reaches large values at low temperatures, which strongly suggests the wide distributions of local susceptibilities χ_j obtained in disorder-driven theories of non-Fermi-liquid (NFL) behavior. The NMR linewidths agree well with distribution functions $P(\chi)$ which fit bulk susceptibility and specific heat data. The apparent return to Fermi-liquid behavior observed below 1 K is manifested in the vanishing of $P(\chi)$ as $\chi \rightarrow \infty$, suggesting the absence of strong magnetic response at low energies. Our results indicate the need for an extension of some current theories of disorder-driven NFL behavior in order to incorporate this low-temperature crossover.

PACS numbers: 71.27.+a, 75.30.Mb, 76.60.Cq.

I. INTRODUCTION

A breakdown of the standard Landau Fermi-liquid theory is signaled in certain heavy-fermion metals by anomalies in thermodynamic, transport, and optical properties at low temperatures and frequencies.¹ Although exceptions exist, the anomalous properties are usually as follows: the Sommerfeld specific heat coefficient $\gamma(T) = C(T)/T$ diverges as $-\ln T$; the magnetic susceptibility $\chi(T)$ varies as $1 - aT^{1/2}$ or diverges as $-\ln T$ or a weak inverse power of temperature; the electrical resistivity departs linearly with temperature from its $T = 0$ value; and optical conductivity experiments in the non-Fermi-liquid (NFL) alloy UCu_{3.5}Pd_{1.5} indicate a transport relaxation rate which varies linearly with frequency at low temperatures.²

Attempts to understand this NFL behavior invoke one or more characteristics common to most such systems, viz., the possibility of an unconventional Kondo effect,^{3,4} proximity to a quantum critical point (QCP),⁵⁻⁷ structural disorder,⁸ or a combination of the latter two.⁹ Recent experimental work has stressed the role that disorder can play. In particular, the observed inhomogeneous broadening of copper nuclear magnetic resonance (NMR) lines in the NFL alloys UCu_{5-x}Pd_x, $x = 1.0$ and 1.5 , could be described by a disorder-induced spatial distribution of local susceptibilities χ_j .^{10,11} Such a susceptibility distribution originates in the interplay between structural disorder and many-body effects intrinsic to f -electron systems, such as the Kondo effect and the Ruderman-Kittel-Kasuya-Yosida (RKKY) interaction between the magnetic moments.

It is clear that if an interaction between moments is present the term “non-Fermi liquid” must be used with care, since strictly speaking Fermi-liquid theory deals only with the lowest-lying excitations of a system of interacting fermions and hence is correct only in the zero-temperature limit in the absence of a phase transition. Any kind of magnetic phase transition or glassy spin freezing at nonzero temperature invalidates this condition, and NFL behavior is no longer a surprise. Following convention in this field, we nevertheless continue to designate as NFL systems materials in which the properties mentioned above are found at intermediate temperatures, with the proviso “nearly NFL” applied if there is evidence for a crossover to a new state at low temperatures.

In this paper we report measurements of the magnetic susceptibility and ²⁹Si NMR linewidth in the nearly-NFL¹² heavy-fermion alloy CeRhRuSi₂, and consider the data in the light of two such disorder-driven scenarios: (1) the so-called “Kondo disorder” picture of Bernal *et al.*¹⁰ and Miranda, Dobrosavljević, and Kotliar,⁸ in which the RKKY interaction is disregarded and the local susceptibility distribution is associated with a corresponding distribution of single-ion Kondo temperatures T_K , and (2) a recent model by Castro Neto and co-workers⁹ based on the existence of quantum Griffiths singularities¹³ in a disordered system with RKKY couplings which is close to a QCP.^{1,6} In the latter case Kondo and RKKY phenomena compete with each other in the random environment, and the susceptibility is associated with fluctuations of magnetic clusters.⁹ Both of these models have been shown to account for the observed susceptibility and NMR broadening in UCu_{5-x}Pd_x,^{9,11} and the Kondo-

disorder model is in agreement with the transport and optical data for $\text{UCu}_{5-x}\text{Pd}_x$ alloys. The Griffiths-phase picture describes the thermodynamic properties of a number of NFL materials.¹⁴

It should be pointed out that NFL mechanisms based on unconventional Kondo effects^{3,4} have to date been treated only for isolated f ions. It would be useful to extend such pictures, first to the case of ordered f -ion-based compounds and then with the inclusion of disorder in analogy with the Griffiths-phase model.

Similarities and differences between the Kondo-disorder and Griffiths-phase theories of NFL behavior and the necessity for their modification at low temperatures are discussed in the light of our experimental data. Fits of the theories to the temperature dependence of the bulk susceptibility determine the parameters of each model, each of which then predicts the temperature dependence and size of the NMR linewidth with no further adjustable parameters. The measured linewidths are in good agreement with both models. This corroborates the conclusion of Graf *et al.*,¹² based on susceptibility and specific heat measurements, that disorder-driven NFL behavior is important in this system.

The isostructural alloy system $\text{Ce}(\text{Ru}_{1-x}\text{Rh}_x)_2\text{Si}_2$ exhibits a variety of complex behavior associated with the Kondo effect and magnetic interactions.^{15–20} The phase diagram of this system^{16–18} is shown in Fig. 1. The

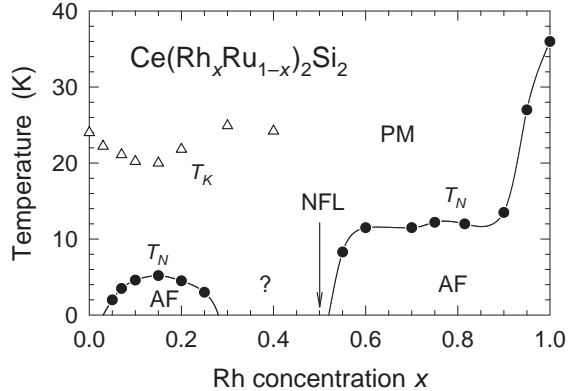


FIG. 1. Magnetic phase diagram of $\text{Ce}(\text{Ru}_{1-x}\text{Rh}_x)_2\text{Si}_2$. Data from Refs. 16–18. Paramagnetic (PM) and antiferromagnetic (AF) regions are indicated. Circles: AF ordering temperatures T_N . Triangles: Kondo temperatures T_K . The curves are guides for the eye. The arrow indicates the concentration for which NFL behavior was observed by Graf *et al.* (Ref. 12).

end compound CeRu_2Si_2 is a heavy-fermion metal which shows no long-range magnetic order down to 20 mK,¹⁵ whereas CeRh_2Si_2 is an antiferromagnet¹⁶ with Néel temperature $T_N = 36$ K. Antiferromagnetism is found for low ($0.1 \lesssim x \lesssim 0.3$) and high ($0.5 \lesssim x \leq 1$) rhodium doping. Neutron diffraction experiments¹⁹ in the low-doping

range show that the antiferromagnetism is incommensurate (i.e., the $4f$ electrons are itinerant), but becomes commensurate, indicative of local moments, for $x \gtrsim 0.5$. For $x \lesssim 0.4$ the specific heat indicates a characteristic energy scale, usually associated with the average Kondo temperature T_K of the material, which is higher than T_N in this composition range.

The concentration $x = 0.5$ is near the critical value for suppression of T_N to zero. In spite of its stoichiometric composition CeRhRuSi_2 is a disordered alloy, as the Rh and Ru atoms occupy the same crystallographic site and there is no evidence of superlattice formation. For $x = 0.5$ Graf *et al.*¹² found the weak divergences characteristic of NFL behavior¹ in $\gamma(T)$ and $\chi(T)$ for temperatures between 1 and 30 K. There was no evidence for magnetic ordering, and Graf *et al.* concluded that NFL phenomena in CeRhRuSi_2 are driven by structural disorder. To our knowledge the region $0.3 \lesssim x \lesssim 0.5$ has not been examined for NFL behavior.

Below 1 K $\gamma(T)$ was seen to saturate, suggesting that CeRhRuSi_2 exhibits a crossover from a region of anomalous magnetic response to a Fermi-liquid ground state as the temperature is lowered. It should be noted, however, that recent specific heat and ac susceptibility studies of $\text{UCu}_{5-x}\text{Pd}_x$ ^{21,22} suggest that saturation of $\gamma(T)$ in this system may be associated with magnetic ordering, possibly of a spin-glass nature or in the form of superparamagnetic clusters. More information on the behavior of NFL systems at low temperatures is clearly needed.

The bulk susceptibility agrees well with the Kondo-disorder model but is overestimated by the Griffiths-phase picture at low temperatures. This is not surprising, since the possibility of nearly-NFL behavior is built into the Kondo-disorder model, whereas the Griffiths-phase theory in its present form neglects effects, such as transverse Kondo fluctuations or residual interactions between clusters, which could modify or remove the Griffiths singularities which cause the NFL behavior.

The experimental data obtained to date do not discriminate clearly between the two pictures, since the distribution function $P(\chi)$ which describes the inhomogeneous distribution of susceptibilities contains no qualitative feature sensitive to the existence of RKKY-coupled clusters. We speculate that dynamical properties such as nuclear spin-lattice relaxation rates may be more sensitive to low-lying excitations associated with spin-spin couplings, particularly at low temperatures, and suggest that further measurements of spin relaxation rates be carried out.

Sec. II of the paper describes our measurements of bulk magnetic susceptibility and ^{29}Si NMR spectra in CeRhRuSi_2 . The relation between inhomogeneity in the susceptibility and the NMR linewidth is reviewed in Sec. III. Sec. IV treats the single-ion Kondo-disorder and Griffiths-phase disorder-driven NFL mechanisms. Analysis of the susceptibility and NMR data is discussed in Sec. V, and Sec. VI gives our conclusions.

II. EXPERIMENT

Measurements of bulk susceptibility and ^{29}Si NMR spectra were carried out on unaligned and field-aligned²³ powder samples of CeRhRuSi_2 at a frequency of 20.220 MHz and temperatures in the range 4.2–230 K. Field-swept NMR spectra were obtained using pulsed-NMR spin-echo signals and the frequency-shifted-and-summed Fourier-transform processing technique described by Clark *et al.*²⁴ The solid curve in Fig. 2 shows a ^{29}Si NMR spectrum from an unaligned powder sample at 4.2 K. We attempted to fit this spectrum to an anisotropic

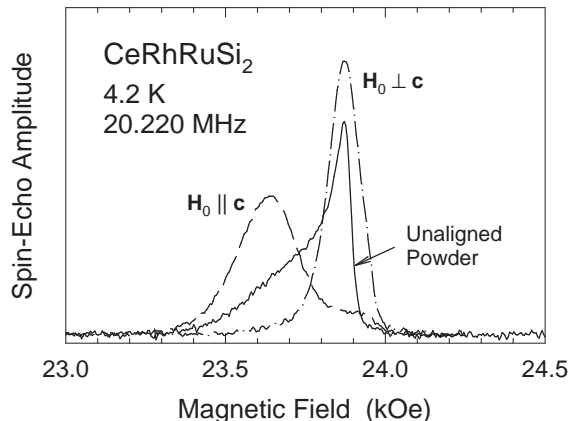


FIG. 2. Field-swept ^{29}Si NMR spectra in CeRhRuSi_2 for $T = 4.2$ K and spectrometer frequency 20.220 MHz. Solid curve: unaligned powder sample. Dashed curve: field-aligned powder, $\mathbf{H}_0 \parallel \mathbf{c}$. Dash-dot curve: field-aligned powder, $\mathbf{H}_0 \perp \mathbf{c}$.

powder pattern²⁵ convoluted with a Gaussian broadening function, but found a poor fit if the width of the broadening is assumed independent of crystallite orientation. The low-field side of the spectrum, which is due to those crystallites with c axes parallel to the applied field \mathbf{H}_0 ($H_0 \approx 24$ kOe), is more strongly broadened than the high-field side. Fits to the low-field region of the spectrum yielded a crude estimate of the extra broadening, which becomes large at low temperatures as predicted by the disorder-driven NFL mechanisms discussed above.

The magnetic susceptibility $\chi(T) = M(H, T)/H$, where $M(H, T)$ is the bulk magnetization of the system, is strongly anisotropic in the $\text{Ce}(\text{Ru}_{1-x}\text{Rh}_x)_2\text{Si}_2$ series, with the c -axis susceptibility $\chi_c(T)$ ($\mathbf{H}_0 \parallel \mathbf{c}$) much larger than the ab -plane susceptibility $\chi_{ab}(T)$ ($\mathbf{H}_0 \perp \mathbf{c}$).¹⁶ This suggests that the extra broadening observed for $\mathbf{H}_0 \parallel \mathbf{c}$ might be due to disorder in the susceptibility similar to that found in $\text{UCu}_{5-x}\text{Pd}_x$, and we were motivated to measure the linewidth in a field-aligned powder sample.²³ The powder was mixed with epoxy, which was allowed to harden in a magnetic field of 60 kOe. The torque on

the anisotropic moment aligned the c axis of each single-crystal powder grain in the direction of the applied field before the epoxy hardened.

The anisotropic susceptibility measured in this field-aligned powder sample is shown in Fig. 3. These data

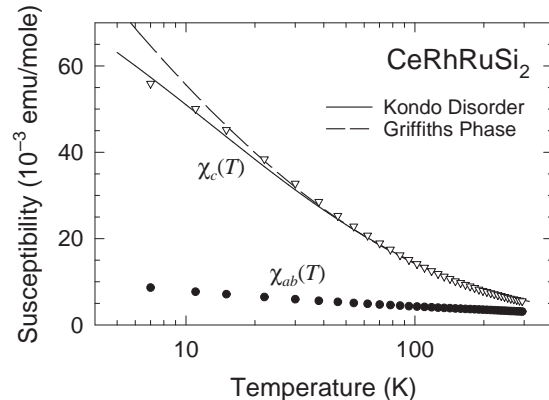


FIG. 3. Temperature dependence of the anisotropic susceptibility in a field-aligned powder sample of CeRhRuSi_2 . Circles: basal-plane susceptibility $\chi_{ab}(T)$. Triangles: c -axis susceptibility $\chi_c(T)$. Solid curve: fit of single-ion Kondo-disorder model (Refs. 10 and 11) to $\chi_c(T)$. Dashed curve: fit of Griffiths-phase model (Ref. 9) to $\chi_c(T)$.

agree well with measurements on a small single crystal of CeRhRuSi_2 (not shown). A strong Curie-Weiss-like temperature dependence is found for $\chi_c(T)$, whereas $\chi_{ab}(T)$ is small and only weakly temperature dependent.²⁶ The curves give fits of $\chi_c(T)$ to the Kondo-disorder and Griffiths-phase models as discussed below in Sects. IV A and IV B, respectively.

Figure 2 also gives the ^{29}Si NMR spectra measured in the field-aligned powder sample for $\mathbf{H}_0 \parallel \mathbf{c}$ and $\mathbf{H}_0 \perp \mathbf{c}$. It can be seen that, as expected, the line is wider for $\mathbf{H}_0 \parallel \mathbf{c}$ than for $\mathbf{H}_0 \perp \mathbf{c}$. The small shoulder on the high-field side of the $\mathbf{H}_0 \parallel \mathbf{c}$ line indicates that the alignment of crystallites in this sample is not perfect. The large linewidth anisotropy implies, however, that neither a small misalignment of the crystallites in the sample nor a slight misalignment of the sample with respect to \mathbf{H}_0 affect linewidth measurements appreciably for $\mathbf{H}_0 \parallel \mathbf{c}$. ^{29}Si NMR spectra from a more completely aligned but smaller sample (not shown) confirmed this expectation. The misalignment does, however, preclude any attempt to obtain information about the shape of $P(\Delta)$ from the shape of the NMR line.

III. SUSCEPTIBILITY INHOMOGENEITY AND NMR LINEWIDTH

Since the NMR frequency shift of a given nucleus is determined by the interaction between its magnetic mo-

ment and those of the surrounding electrons, any spatial variation of the electronic magnetic susceptibility will be reflected in the NMR linewidth as a distribution of frequency shifts. A quantitative understanding of the susceptibility inhomogeneity requires analysis of the relation between it and the NMR linewidth, independent of the particular mechanism which causes the inhomogeneity.

The NMR frequency shift K measures the time-averaged effective field produced by the local moment at the resonating nucleus. In a paramagnet the relative shift K_i of the i^{th} nucleus is related to the local susceptibility χ_j associated with the j^{th} f -ion electronic moment by²⁵

$$K_i = \sum_j a_{ij} \chi_j, \quad (1)$$

where a_{ij} is the hyperfine coupling constant between the j^{th} moment and the i^{th} nucleus. It is straightforward to carry out the spatial averages and show that

$$\overline{K} = a\overline{\chi}, \quad a \equiv \sum_j a_{ij},$$

where a bar designates a spatial average in this and the following. Similarly, the rms spread of shifts $\delta K \equiv (\overline{K^2} - \overline{K}^2)^{1/2}$ is related to the corresponding rms spread of susceptibilities $\delta\chi$ by

$$\delta K = a^* \delta\chi,$$

where a^* is an effective hyperfine coupling constant, discussed in more detail below. As a consequence

$$\delta\chi/\overline{\chi} = \delta K/(a^*\overline{\chi}). \quad (2)$$

If each nucleus is coupled to more than one moment [cf. Eq. (1)], any spatial correlation between the moment susceptibilities will affect the value of a^* . There are two extreme limits in considering this spatial correlation. The term ‘‘long-range correlation’’ (LRC) will be used to describe the situation where the correlation length between local moments is much longer than the local-moment near-neighbor spacing. Similarly, ‘‘short-range correlation’’ (SRC) describes the situation where the variation of susceptibility from site to site is random or nearly so, i.e., where the correlation length which describes this variation is of the order of or shorter than a lattice constant. Note that this correlation is only a phenomenological description of the inhomogeneous susceptibility, and is not necessarily related to critical behavior of the system. For a given system we do not know *a priori* which (if either) of these limits is applicable, although in the single-ion Kondo-disorder model we might expect that random ligand disorder would lead to relatively short-range correlation.

It can be shown¹¹ that the values of a^* in the LRC and SRC limits (denoted by a_{LRC}^* and a_{SRC}^* , respectively) are given by

$$a_{\text{LRC}}^* = |a|; \quad a_{\text{SRC}}^* = \left(\sum_j a_{ij}^2 \right)^{1/2}.$$

Assuming for simplicity that the hyperfine coupling is predominantly to an effective number n_{eff} of f -ion near neighbors and is the same effective value a_{eff} for each of these neighbors, it follows that

$$a_{\text{SRC}}^* = \sqrt{n_{\text{eff}}} a_{\text{eff}} \quad \text{and} \quad a_{\text{LRC}}^* = n_{\text{eff}} a_{\text{eff}},$$

so that

$$a_{\text{SRC}}^* = a_{\text{LRC}}^* / \sqrt{n_{\text{eff}}}. \quad (3)$$

In the LRC limit the fractional susceptibility inhomogeneity $\delta\chi/\overline{\chi}$ is given by the relative NMR linewidth $\delta K/|\overline{K}|$. Since $\delta K = \sigma/H_0$, where σ is the rms linewidth in magnetic field units, we have from Eq. (2)

$$\begin{aligned} \frac{\delta\chi}{\overline{\chi}} &= \frac{\delta K}{a_{\text{LRC}}^* \overline{\chi}} = \frac{\delta K}{|\overline{K}|} \\ &= \frac{\sigma}{|\overline{K}| H_0} \quad (\text{LRC limit}). \end{aligned} \quad (4)$$

Thus $\sigma/(|\overline{K}| H_0)$, which can be derived from the NMR data, is an estimator for $\delta\chi/\overline{\chi}$ in the LRC limit. The corresponding estimator in the SRC limit can be obtained from $\sigma/(|\overline{K}| H_0)$ simply by scaling by the factor $\sqrt{n_{\text{eff}}}$ [Eq. (3)]:

$$\begin{aligned} \frac{\delta\chi}{\overline{\chi}} &= \frac{\delta K}{a_{\text{SRC}}^* \overline{\chi}} = \left(\frac{\delta K}{|\overline{K}|} \right) \left(\frac{a_{\text{LRC}}^*}{a_{\text{SRC}}^*} \right) \\ &= \sqrt{n_{\text{eff}}} \left(\frac{\delta K}{|\overline{K}|} \right) \quad (\text{SRC limit}). \end{aligned} \quad (5)$$

The above assumes that the coupling constants a_{ij} are not disordered, i.e., that they have the same values for crystallographically equivalent positions of nucleus i and f -ion j . If this is not the case and the a_{ij} are also disordered, then it can be shown¹¹ that

$$\frac{\delta K}{|\overline{K}|} = \left[\left(\frac{\delta\chi}{\overline{\chi}} \right)^2 + A^2 \right]^{1/2}, \quad (6)$$

where A is a term which expresses the effect of the disordered a_{ij} . Now in existing disorder-driven models^{10,8,9} it is found that $\delta\chi/\overline{\chi}$ varies considerably with $\overline{\chi}$ (with temperature an implicit parameter), tending to a value $\gtrsim 1$ at low temperatures and vanishing as $\overline{\chi} \rightarrow 0$ (high temperatures). On the other hand A is found to be independent of $\overline{\chi}$. Disorder in the a_{ij} will therefore result in a nonzero intercept in a plot of $\delta K/|\overline{K}|$ vs. $\overline{\chi}$, and its effect can be removed by subtracting this intercept in quadrature from the raw $\delta K/|\overline{K}|$ data. It can be shown that this correction is valid in both the LRC limit and the SRC limit.

It should be stressed that this ‘‘NMR technology’’ is quite independent of the specific mechanism which causes the susceptibility inhomogeneity.

IV. DISORDER-DRIVEN NFL MECHANISMS

In considering systems where NFL behavior is driven by disorder it is convenient to study the spatially-distributed local susceptibility χ_j . Simple linear response theory shows that the zero-temperature local susceptibility can be associated with a characteristic local energy scale Δ_j by

$$\chi_j \propto \frac{1}{\Delta_j}, \quad (7)$$

where Δ_j is essentially the excitation energy from the ground state to the first excited state. At finite temperatures T the local susceptibility $\chi(\Delta, T)$ depends strongly on the microscopic details which couple the magnetic degrees of freedom.

We can therefore speak of distributions of susceptibilities or energy scales, characterized by distribution functions $P(\Delta)$ and $P(\chi)$, respectively; thus $P(\chi, T) = P(\Delta)/|\partial\chi(\Delta, T)/\partial\Delta|$. Once $P(\Delta)$ [or $P(\chi, T)$] is known we can obtain spatial averages of physical quantities such as the n^{th} moment $\bar{\chi}^n(T)$ of the local susceptibility distribution, which is given by

$$\bar{\chi}^n(T) = \int_0^\infty \chi^n(\Delta, T) P(\Delta) d\Delta \quad (8a)$$

$$= \int_0^\infty \chi^n P(\chi, T) d\chi. \quad (8b)$$

Knowledge of the first and second moments of $P(\chi, T)$ is sufficient for interpretation of the bulk susceptibility and NMR linewidth data.

A. Single-ion Kondo disorder

We take the Ce-ion spins to be coupled to the conduction-electron spins by a s - f exchange coupling described by a coupling constant $g = N(E_F)J$, where $N(E_F)$ is the density of conduction-electron states at the Fermi surface and J is the Ce-ion-conduction-electron exchange interaction. If the system is disordered on the ligand sites, as in CeRhRuSi₂, g will be randomly distributed according to a distribution function $P(g)$. In the simplest picture of the Kondo effect, the Kondo temperature T_K , which characterizes the energy scale of the single-ion Kondo effect, is given by $T_K = E_F e^{-1/g}$, where E_F is the Fermi energy. Thus a narrow distribution of g can lead to a wide distribution of T_K when g is small. In this picture we immediately identify Δ with T_K .

If the distribution function $P(\Delta) = P(T_K)$ is broad enough so that $P(T_K \rightarrow 0)$ does not vanish, then at any nonzero temperature T those f ions for which $T_K < T$ are not compensated (i.e., are not described by Fermi-liquid theory) and give rise to the NFL behavior. In

view of Eq. (7) one sees that regions of the system where T_K is very small (sites with very large low-temperature susceptibility) dominate the thermal and transport properties. Miranda *et al.*⁸ have treated this picture in detail, and have shown that it predicts the observed low-temperature behavior of the Sommerfeld coefficient $\gamma(T)$, susceptibility $\chi(T)$, and resistivity $\Delta\rho(T) = \rho(T) - \rho(0)$ ($\gamma \propto \chi \propto -\ln T$ and $\Delta\rho \propto T$, respectively) provided that $P(T_K \rightarrow 0)$ is finite.

The resulting distribution function $P(T_K)$ is given by

$$P(T_K) = P(g) \left| \frac{dg}{dT_K} \right| = \frac{g^2 P(g)}{T_K} \quad (9)$$

with $g = 1/\ln(E_F/T_K)$. As a convenient parameterization of the Kondo physics we take the susceptibility to have the Curie-Weiss form

$$\chi(T, T_K) = \mathcal{C}/(T + \alpha T_K), \quad (10)$$

where \mathcal{C} is the Curie constant. The value of α was estimated by comparing this Curie-Weiss law to the exact Bethe-ansatz solution;²⁷ the two functional forms differ by $\lesssim 10\%$ for $\alpha \approx 2.5$. Assuming a Gaussian distribution for $P(g)$, the mean \bar{g} and rms width δg of the distribution can be found by fitting Eq. (8) with $n = 1$ to the measured bulk (i.e., spatially averaged) susceptibility.^{10,12}

B. Griffiths-phase model

In the Griffiths-phase model of NFL behavior⁹ the low-energy physics is dominated by rare and large clusters which can tunnel over classically forbidden regions. These correlated regions are generated by above-average values of the RKKY interaction. The tunneling is produced by the spin-flip processes present in the Kondo effect.⁹ In this scenario the Griffiths singularities appear close to a QCP below percolation threshold and are therefore intrinsically related to QCP physics. It is intuitively clear that the clusters can be effectively described in terms of two level systems, with tunneling energy E which is distributed over the sample due to the structural disorder. Obviously we have $\Delta = E$ in this picture.

The distribution of E is obtained by mapping the problem onto the Ising model in a transverse field; this procedure is valid in the limit of large magnetic anisotropy as appears to be the case in CeRuRhSi₂ (cf. Fig. 3). Then it can be shown²⁸ that

$$P(E) = \begin{cases} \frac{\lambda}{\epsilon_0} \left(\frac{E}{\epsilon_0} \right)^{-1+\lambda}, & 0 < E < \epsilon_0, \\ 0, & E > \epsilon_0, \end{cases} \quad (11)$$

where λ is an exponent that determines the behavior of the response functions ($0 \leq \lambda \leq 1$), and ϵ_0 is a high energy cut-off which must be determined for each specific system.

As discussed above the local zero-temperature susceptibility in this picture is $\chi(0, E) = \mathcal{C}/E$; large clusters with small energy scales have large susceptibilities. At high temperatures one expects the clusters to be disordered and behave paramagnetically, resulting in a Curie behavior $\chi(E, T) = \mathcal{C}/T$ for $T \gg E$. We therefore assume a Curie-Weiss interpolation formula

$$\chi(E, T) = \frac{\mathcal{C}}{T + E} \quad (12)$$

as for the Kondo-disorder model. But in the present case this approximation is intended to incorporate all the interaction effects which determine the susceptibility of a multi-ion cluster, not just single-ion Kondo physics.

Using Eqs. (8), (11), and (12) it is straightforward to show²⁸ that for $T \ll \epsilon_0$

$$\bar{\chi}(T) = \frac{\pi\lambda\mathcal{C}}{\epsilon_0} \left(\frac{\epsilon_0}{T}\right)^{1-\lambda} \quad (13)$$

and

$$\frac{\delta\chi(T)}{\bar{\chi}(T)} = \left[\frac{1-\lambda}{2\pi\lambda}\right]^{1/2} \left(\frac{\epsilon_0}{T}\right)^{\lambda/2}. \quad (14)$$

The critical behavior is determined by the single nonuniversal temperature-independent exponent λ . For $\lambda < 1$ the susceptibility diverges algebraically as $T \rightarrow 0$ ($H = 0$), and NFL behavior is obtained. The divergence increases (i.e., the NFL behavior becomes stronger) with decreasing λ . The case $\lambda = 1$ is marginal, and leads to logarithmic singularities as in the Kondo-disorder approach.⁸

C. Kondo disorder versus Griffiths singularities

Both the Kondo-disorder and Griffiths-singularities pictures deal with a similar aspect of disorder, viz., the physics of rare events with large susceptibilities. It is clear, however, that the microscopic aspects of the two models are very different. The Kondo-disorder model uses non-interacting single-ion physics, and no aspect of the RKKY interaction is present. The Griffiths-phase approach, on the other hand, tries to take both RKKY and Kondo phenomena into account on an equal footing, and has a strong connection with QCP physics.

From the point of view of local properties as measured in NMR spectra these approaches give similar results. The spatial properties of the two approaches are very different, however, since the formation of clusters in the Griffiths phase requires spatially extended structure. In this case one could look for the existence of clusters via superparamagnetic response, which is well understood in the context of spin glasses,²⁹ or for a momentum dependence of the inelastic neutron scattering. In addition, one would expect cluster formation to slow down the spin fluctuations relative to the free-ion fluctuation rate,

which is essentially T_K . Experiments that are sensitive to the fluctuation rate may therefore be able to distinguish between the two theories.

V. RESULTS AND DISCUSSION

A. Bulk magnetic susceptibility

A fit of the Kondo-disorder model result for $\bar{\chi}(T)$ [Eq. (8) with $n = 1$ and $\Delta = T_K$, and Eqs. (9) and (10) for $P(T_K)$ and $\chi(T, T_K)$] to the experimental c -axis susceptibility $\chi_c(T)$ is shown as the solid curve in Fig. 3. We obtain the same coupling constant distribution width $\delta g = 0.021$ as Graf *et al.*,¹² and a somewhat smaller mean $\bar{g} = 0.160$ compared to 0.175 from Ref. 12.³⁰ The coupling constants are less widely distributed than in the NFL system $\text{UCu}_{5-x}\text{Pd}_x$, $x = 1.0$ and 1.5,¹¹ consistent with weaker “nearly NFL” behavior in CeRhRuSi_2 .

Figure 3 also gives the Griffiths-phase model prediction for $\chi_c(T)$ (dashed curve), obtained by fitting $\bar{\chi}(T)$ from Eq. (8) ($n = 1$), with $\Delta = E$ and using Eqs. (11) and (12), to the bulk c -axis susceptibility. The best fit is given by the dashed curve in Fig. 3. It can be seen that at low temperatures the Griffiths-phase fit curve overestimates the experimental data slightly. This is to be expected, since in the simple Griffiths-phase model there is no possibility of a return to Fermi-liquid behavior at low temperatures: the system is a true NFL as long as $\lambda < 1$. But the susceptibility data begin to exhibit the saturation expected from the conclusions of Graf *et al.*,¹² and therefore are not well described by an algebraically divergent temperature dependence. There is, however, a region of intermediate temperatures in which both Kondo-disorder and Griffiths-singularity models agree very well with experiment. From the Griffiths-phase fit in this region we obtain $\epsilon_0 = 170 \pm 10$ K and $\lambda = 0.88 \pm 0.02$. The latter value is considerably larger (i.e., the NFL behavior is weaker) than found in $\text{UCu}_{5-x}\text{Pd}_x$ ⁹ as in the Kondo disorder model.

Figure 4 shows the distribution functions $P(\Delta)$ which result from the Kondo-disorder ($\Delta = T_K$) and Griffiths-phase ($\Delta = E$) model fits. It can be seen that the two functions are very different. The Kondo-disorder distribution function $P(T_K)$ exhibits a maximum near 12 K and is small below ~ 1 K and above ~ 100 K, whereas the Griffiths-phase distribution function $P(E)$ is broader and diverges weakly as $E \rightarrow 0$. These differences are much more marked in $P(\Delta)$ than in the corresponding fits to the susceptibility (Fig. 3); spatially-averaged experimental quantities are insensitive to the exact form of $P(\Delta)$. It is clear that the Griffiths-phase model could fit the data better if $P(E) \rightarrow 0$ as $E \rightarrow 0$, which in an extended Griffiths-phase picture would occur if there were an upper cutoff on the cluster susceptibility.

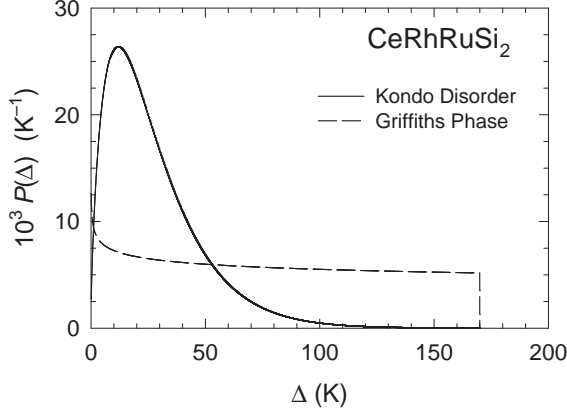


FIG. 4. Distribution functions $P(\Delta)$ of characteristic energies Δ in CeRhRuSi_2 , obtained from fitting the Kondo-disorder ($\Delta = T_K$) and Griffiths-phase ($\Delta = E$) models to the bulk c -axis susceptibility (Fig. 3). Solid curve: Kondo-disorder distribution function $P(T_K)$ [Eq. (9)]. Dashed curve: Griffiths-phase distribution function $P(E)$ [Eq. (11)].

Thus CeRhRuSi_2 does not exhibit “true” NFL behavior. In the Kondo-disorder model, which shows this most explicitly, the best fit indicates that all spins are in a Kondo-compensated Fermi-liquid state at low enough temperatures. This is consistent with the results of Graf *et al.*¹² that $\gamma(T) \rightarrow \text{const.}$ and $\Delta\rho(T) \propto T^2$ as $T \rightarrow 0$. We note again, however, that as mentioned in Sec. I the saturation of $\gamma(T)$ does not necessarily indicate Fermi-liquid behavior at low temperatures; other physics, such as magnetic freezing,^{21,22} may be involved.

B. ^{29}Si NMR linewidths

The ^{29}Si c -axis NMR shift K_c and linewidth σ_c are plotted against the c -axis bulk susceptibility χ_c in Fig. 5, with temperature an implicit parameter. (The ab -plane parameters K_{ab} and σ_{ab} , not shown, are small and only weakly temperature dependent.) It can be seen that σ_c varies more rapidly with χ_c than K_c , as expected qualitatively from disorder-driven theories of NFL behavior.^{8–10} Although the expected linear relation between K_c and χ_c is observed at high temperatures (small χ_c), $K_c(\chi_c)$ tends to a constant for large χ_c . This saturation is not well understood, but may be due to a small amount of second phase; this could have a strong Curie-Weiss-like susceptibility but little effect on the NMR shift since the number of nuclei in the second phase would be small.³¹ The observed nonlinearity is not more than $\sim 20\%$ and does not affect our conclusions significantly.

Figure 6 plots $\sigma_c/(K_c H_0) = \delta K_c/K_c = \delta K_c/(a_{\text{LRC}}^* \chi_c)$ [Eq. (4)] versus χ_c . As discussed in Sec. III $\sigma_c/(K_c H_0)$

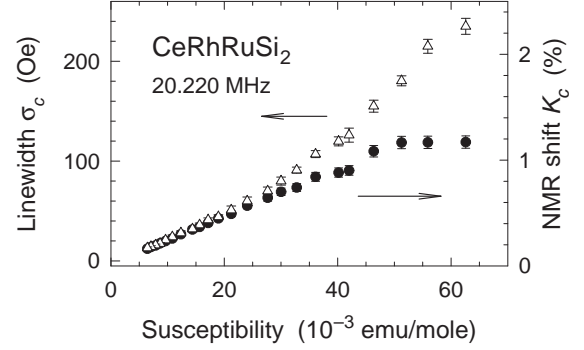


FIG. 5. ^{29}Si c -axis NMR shift K_c (circles) and linewidth σ_c (triangles) vs. c -axis susceptibility χ_c in CeRhRuSi_2 , with temperature an implicit parameter. Spectrometer frequency 20.220 MHz (applied field ~ 23.9 kOe). The linewidth σ_c varies more rapidly with χ_c than K_c , as expected from disorder-driven theories of NFL behavior (Refs. 8–10).

is an estimator for $\delta\chi/\bar{\chi}$ in the LRC limit. The data extrapolate to a non-zero value as $\chi_c \rightarrow 0$, which indicates that the coupling constant a_{ij} is also disordered. We therefore subtracted the extrapolated intercept from the raw values in quadrature [cf. Eq. (6)] to obtain corrected data in the LRC limit, also shown in Fig. 6 (triangles). These corrected data represent $\delta K_c/(a_{\text{LRC}}^* \chi_c)$ with δK_c due only to susceptibility inhomogeneity. The corresponding (corrected) values of $\delta K_c/(a_{\text{SRC}}^* \chi_c)$ were obtained from Eq. (5) of Sec. III, with n_{eff} chosen as described below.

For both the Kondo-disorder and Griffiths-phase models $\delta\chi/\bar{\chi}$ was calculated from Eq. (8) ($n = 2$) and $\bar{\chi}(T)$ with no further adjustable parameters, since $P(\Delta)$ had been previously determined by the fits to the bulk susceptibility. Figure 7 compares $\delta K_c/(a^* \chi_c)$ in both limits with the theoretical behavior of $\delta\chi/\bar{\chi}$ from these theories, again with temperature an implicit parameter. It can be seen that the theoretical predictions are similar and that they both overestimate $\delta K_c/(a_{\text{LRC}}^* \chi_c)$ considerably, but that the agreement with $\delta K_c/(a_{\text{SRC}}^* \chi_c)$ is excellent when n_{eff} in Eq. (5) is taken to be 6.

That this value is sensible can be concluded from examination of the Al_4Ba -type crystal structure of CeRhRuSi_2 , shown in Fig. 8, where it can be seen that each Si site is coordinated by four Ce nearest neighbors and one Ce next-nearest neighbor. Thus n_{eff} is approximately the coordination number for the first two near-neighbor shells and is therefore reasonable, given the approximation of an effective number of equally-coupled neighbors.

For CeRhRuSi_2 we do not have the independent verification of the SRC limit that was available from comparison of NMR and muon spin rotation (μSR) spectra in the case of $\text{UCu}_{5-x}\text{Pd}_x$.³² (For a review of the

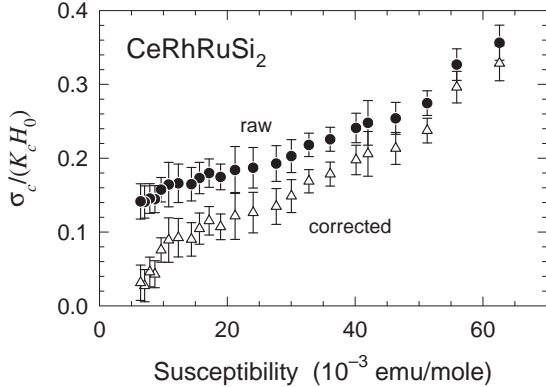


FIG. 6. Plot of relative spread $\sigma_c/(K_c H_0)$ of c -axis ^{29}Si NMR shifts in LRC limit versus c -axis susceptibility χ_c in CeRhRuSi_2 . See text for symbol definitions. Circles: raw data before correction for disorder in the hyperfine coupling constant. Triangles: data corrected for coupling constant disorder (see text).

μSR technique see, for example, Ref. 33.) The latter alloys have a cubic crystal structure and the positive-muon (μ^+) interstitial stopping sites possess octahedral and tetrahedral point symmetries, which are sufficiently high to render the μ^+ frequency shift isotropic. Then the μ^+ linewidth reflects the susceptibility inhomogeneity rather than anisotropic powder-pattern broadening. Preliminary μSR measurements in an unaligned powder sample of CeRhRuSi_2 ³⁴ show that in this alloy the anisotropic contribution dominates the powder-pattern linewidth, much as in the unaligned-powder spectrum of Fig. 2, and the disorder-induced broadening cannot be determined accurately.

Unfortunately field-aligned powder samples cannot be used in μSR experiments. The packing fraction of the powder must be small ($\lesssim 20\%$) in order to allow free rotation of the powder grains during alignment, and then only a correspondingly small fraction of the muons stop in the sample; the rest stop in the epoxy and give a spurious signal. Thus we cannot confirm the SRC limit by comparing results between NMR and μSR . We also note that no other nucleus in CeRhRuSi_2 is favorable for NMR; stable Ce isotopes possess no nuclear magnetic moment, and Ru and Rh isotopes have very small gyromagnetic ratios. Nevertheless, the SRC-limit estimate of $\delta\chi_c/\chi_c$ is in excellent self-consistent agreement with the disorder-driven models.

VI. CONCLUSIONS

The picture that emerges from our ^{29}Si NMR study of CeRhRuSi_2 exhibits similarities and differences when compared to the preceding NMR investigation of

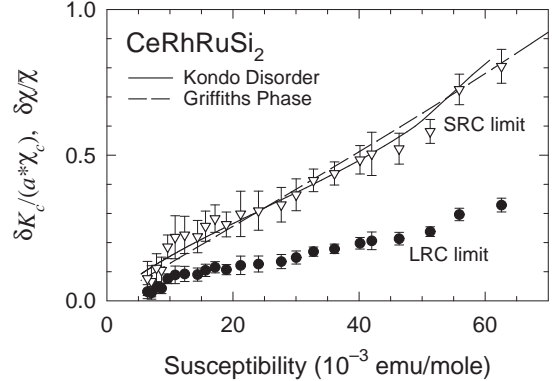


FIG. 7. Experimental and theoretical relations between rms susceptibility inhomogeneity and bulk susceptibility in CeRhRuSi_2 . Data points: c -axis NMR estimator $\delta K_c/(a^* \chi_c)$ of relative rms susceptibility spread $\delta\chi/\bar{\chi}$. Circles: LRC limit (see text). Triangles: SRC limit. Solid curve: $\delta\chi/\bar{\chi}$ in the single-ion Kondo-disorder model. Dashed curve: $\delta\chi/\bar{\chi}$ in the Griffiths-phase model. Agreement is found between predictions of disorder-driven NFL theories and data in the SRC limit for effective nearest-neighbor number $n_{\text{eff}} = 6$.

$\text{UCu}_{5-x}\text{Pd}_x$, $x = 1.0$ and 1.5 .^{10,11} The most important similarity is the fact that in both cases the NMR data are in excellent agreement with predictions of disorder-driven theories of NFL behavior. Our results therefore confirm the conclusions of Graf *et al.*¹² that such a mechanism drives NFL properties in CeRhRuSi_2 . The most important differences between the two systems are that in CeRhRuSi_2 (1) within the single-ion Kondo-disorder model the disorder is not enough to prevent a return to Fermi-liquid behavior at temperatures $\lesssim 1$ K, and (2) the determination of the appropriate correlation length limit (LRC or SRC) has not been made independently of comparison with theory. The agreement between theory and experiment assuming the SRC limit (Fig. 7) is satisfactory.

From the experimental point of view, the relatively small differences between the predictions of the single-ion Kondo-disorder picture and the Griffiths-phase theory show how difficult it is to discriminate between these two mechanisms for disorder-driven NFL behavior in the NMR linewidths. We speculate, however, that the dynamics of the spins will be quite different in the two cases, particularly at low temperatures.

The single-ion Kondo disorder model predicts inhomogeneous relaxation due to the distributed T_K . This mechanism yields a spatially averaged spin-lattice relaxation rate $\overline{T_1^{-1}(T)} = \int dT_K P(T_K) T_1^{-1}(T, T_K)$. It is convenient to approximate $T_1^{-1}(T, T_K)$ by

$$T_1^{-1}(T, T_K) \propto \begin{cases} 1/T_K, & T > T_K, \\ T/T_K^2, & T < T_K, \end{cases}$$

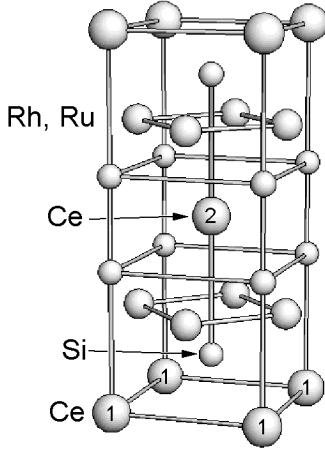


FIG. 8. Crystal structure of $\text{Ce}(\text{Rh}_{1-x}\text{Ru}_x)\text{Si}_2$. Each Si site is coordinated by four Ce nearest neighbors (no. 1) in the adjacent basal plane and one Ce next-nearest neighbor (no. 2) in the opposite basal plane.

which captures the crossover to Fermi-liquid (Korringa) behavior for $T < T_K$. For a model rectangular $P(T_K)$ given by

$$P(T_K) = \begin{cases} \frac{1}{T_M - T_m}, & T_m < T_K < T_M, \\ 0, & \text{otherwise,} \end{cases}$$

where T_m and T_M are minimum and maximum values of T_K , respectively, it is straightforward to show that $\overline{T_1^{-1}}$ varies linearly with T for $T < T_m$ and goes smoothly to a constant for $T > T_M$. Such behavior would be generally expected to characterize $\overline{T_1^{-1}}$ as long as $P(T_K \rightarrow 0) = 0$. Thus in this scenario $\overline{T_1^{-1}}$ depends on temperature but is independent of resonance frequency ω .

In contrast, it can be easily shown from the expression for the dissipative dynamic susceptibility $\chi''(\omega)$ in the Griffiths-phase theory⁹

$$\chi''(\omega) \propto \omega^{-1+\lambda} \tanh(\hbar\omega/k_B T)$$

that, assuming the validity of this picture for the very low nuclear (muon) frequencies ($\hbar\omega \ll k_B T$)

$$\overline{T_1^{-1}} \propto \omega^{-1+\lambda},$$

independent of temperature. The frequency is given by $\omega = \gamma H_0$, where γ is the nuclear (muon) gyromagnetic moment. Thus the dependence of $\overline{T_1^{-1}}$ on temperature and H_0 differs considerably between the two theories.

It should be noted that the NMR linewidths obtained from experimental data are not necessarily true sample rms averages, if the lines have extended shoulders which are lost in the noise and not taken into account. The fact that good fits are obtained with Gaussian lines seems to make this unlikely, but it is not hard to see that at low

temperatures $P(\chi)$ should be broad and asymmetric in both the Kondo-disorder and Griffiths-phase models. If the experimental linewidth characterizes only “typical” environments it will underestimate the true sample average. This would render our quantitative results somewhat uncertain, but would not invalidate the conclusion that disorder is an important element in the NFL behavior of CeRhRuSi_2 above 1 K.

Finally, we discuss the relation of the disorder-driven theories to the observed crossover to a new regime (Fermi-liquid behavior, cluster formation, magnetic freezing, etc.) in CeRuRhSi_2 below 1 K. The crossover is described empirically by the Kondo-disorder model, which by itself gives no clue as to why there should (or should not) be a suppression of low Kondo temperatures. Recently, however, Miranda and Dobrosavljić³⁵ have reported a microscopic calculation of the form of $P(T_K)$ for various levels of disorder. They find that the distribution is singular only for sufficiently strong disorder, whereas for slightly weaker disorder $P(T_K) \rightarrow 0$ at small T_K , consistent with a return to Fermi-liquid behavior at the lowest temperatures. This feature is in at least qualitative agreement with our results.

To explain the crossover the Griffiths-phase scenario would have to be extended beyond its simplest form to include a mechanism which reduces the response of the largest clusters. The mechanism behind such a reduction could be the breakdown of the assumption of strong single-ion anisotropy made in the Griffiths-phase theory;²⁸ transverse fluctuations of the Ce ions might constitute a damping mechanism which rounds off the Griffiths singularities. Alternatively, superparamagnetic spin freezing of the clusters could occur at very low temperatures.^{21,22}

It is possible that similar crossovers occur in other NFL materials, perhaps at temperatures which have not yet been explored. In any event, our experimental findings indicate that further development of current theories of disorder-driven NFL behavior is required to understand NFL phenomena at low temperatures.

One of us (D.E.M.) is grateful for discussions with C. H. Booth, R. H. Heffner, M. F. Hundley, and R. Modler. This research was supported by the U.S. NSF, Grant no. DMR-9418991 (U.C. Riverside), by the Research Corporation (Whittier College), and by the U.C. Riverside Academic Senate Committee on Research, and was performed in part under the auspices of the U.S. DOE (Los Alamos). One of us (A.H.C.N.) acknowledges support from the Alfred P. Sloan Foundation.

¹ See, for example, articles in *Proceedings of the Conference on Non-Fermi Liquid Behavior in Metals*, Santa Barbara,

- California, 1996, edited by P. Coleman, M. B. Maple, and A. J. Millis, *J. Phys.: Condens. Matter* **8** (1996).
- ² L. Degiorgi and H. R. Ott, *J. Phys.: Condens. Matter* **8**, 9901 (1996).
 - ³ D. L. Cox, *Phys. Rev. Lett.* **59**, 1240 (1987).
 - ⁴ I. Affleck and A. W. W. Ludwig, *Nucl. Phys. B* **360**, 641 (1991).
 - ⁵ M. A. Continentino, *Phys. Rev. B* **47**, 11587 (1993).
 - ⁶ A. J. Millis, *Phys. Rev. B* **48**, 7183 (1993).
 - ⁷ A. M. Tselik and M. Reizer, *Phys. Rev. B* **48**, 9887 (1993).
 - ⁸ E. Miranda, V. Dobrosavljević, and G. Kotliar, *J. Phys.: Condens. Matter* **8**, 9871 (1996).
 - ⁹ A. H. Castro Neto, G. Castilla, and B. A. Jones, *Phys. Rev. Lett.* **81**, 3531 (1998).
 - ¹⁰ O. O. Bernal, D. E. MacLaughlin, H. G. Lukefahr, and B. Andraka, *Phys. Rev. Lett.* **75**, 2023 (1995).
 - ¹¹ D. E. MacLaughlin, O. O. Bernal, and H. G. Lukefahr, *J. Phys.: Condens. Matter* **8**, 9855 (1996).
 - ¹² T. Graf, J. D. Thompson, M. F. Hundley, R. Movshovich, Z. Fisk, D. Mandrus, R. A. Fisher, and N. E. Phillips, *Phys. Rev. Lett.* **78**, 3769 (1997).
 - ¹³ R. B. Griffiths, *Phys. Rev. Lett.* **23**, 17 (1969).
 - ¹⁴ M. C. de Andrade, R. Chau, R. P. Dickey, N. R. Dilley, E. J. Freeman, D. A. Gajewski, M. B. Maple, R. Movshovich, A. H. Castro Neto, G. E. Castilla, and B. A. Jones, *Phys. Rev. Lett.* **81**, 5620 (1998).
 - ¹⁵ P. Haen, J. Flouquet, F. Lapierre, P. Lejay, and G. Remenyi, *J. Low Temp. Phys.* **67**, 391 (1987).
 - ¹⁶ B. Lloret, B. Chevalier, B. Buffat, J. Etourneau, S. Quezel, A. Lamharrar, J. Rossat-Mignod, R. Calemczuk, and E. Bonjour, *J. Magn. Magn. Mat.* **63-64**, 85 (1987).
 - ¹⁷ T. Sakakibara, C. Sekine, H. Amitsuka, and Y. Miyako, *J. Magn. Magn. Mat.* **108**, 193 (1992).
 - ¹⁸ C. Sekine, T. Sakakibara, H. Amitsuka, Y. Miyako, and T. Goto, *J. Phys. Soc. Jpn.* **61**, 4536 (1992).
 - ¹⁹ S. Kawarazaki, Y. Kobashi, J. A. Fernandez-Baca, S. Murayama, Y. Onuki, and Y. Miyako, *Physica (Amsterdam) B* **206-207**, 298 (1995).
 - ²⁰ K. Matsuhira, T. Sakakibara, and H. Amitsuka, *Physica (Amsterdam) B* **206-207**, 326 (1995).
 - ²¹ R. Volmer, S. Mock, T. Pietrus, H. v. Löhneysen, R. Chau, and M. B. Maple, *Physica (Amsterdam) B* **230-232**, 603 (1997).
 - ²² E.-W. Scheidt, T. Schreiner, K. Heuser, S. Koerner, and G. R. Stewart, *Phys. Rev. B* **58**, R10104 (1998).
 - ²³ D. E. Farrell, B. S. Chandrasekhar, M. R. McGuire, M. M. Fang, V. G. Kogan, J. R. Clem, and D. K. Finnemore, *Phys. Rev. B* **36**, 4025 (1987).
 - ²⁴ W. G. Clark, M. E. Hanson, F. Lefloch, and P. Segransan, *Rev. Sci. Instrum.* **66**, 2453 (1995).
 - ²⁵ G. C. Carter, L. H. Bennett, and D. J. Kahan, *Metallic Shifts in NMR*, *Prog. Mat. Sci.* **20**, 1 (1977).
 - ²⁶ The small upturn of $\chi_{ab}(T)$ at low temperatures could result from slight misalignment of the powder grains.
 - ²⁷ V. T. Rajan, J. H. Lowenstein, and N. Andrei, *Phys. Rev. Lett.* **49**, 497 (1982).
 - ²⁸ A. H. Castro Neto, G. Castilla, and B. A. Jones (unpublished).
 - ²⁹ J. A. Mydosh, *Spin Glasses: An Experimental Introduction* (Taylor & Francis, London, 1993).
 - ³⁰ It should be noted that Graf *et al.* analyzed susceptibility data from a randomly-oriented powder sample, whereas our results are from a fit to the *c*-axis susceptibility of a field-aligned powder.
 - ³¹ D. E. MacLaughlin, *J. Magn. Magn. Mat.* **47**, 121 (1985).
 - ³² O. O. Bernal, D. E. MacLaughlin, A. Amato, R. Feyherm, F. N. Gygax, A. Schenck, R. H. Heffner, L. P. Le, G. J. Nieuwenhuys, B. Andraka, H. von Löhneysen, O. Stockert, and H. R. Ott, *Phys. Rev. B* **54**, 13000 (1996).
 - ³³ A. Schenck, *Muon Spin Rotation Spectroscopy: Principles and Applications in Solid State Physics* (A. Hilger, Bristol & Boston, 1985).
 - ³⁴ D. E. MacLaughlin, R. H. Heffner, L. P. Le, J. D. Thompson, Z. Fisk, G. J. Nieuwenhuys, A. Amato, A. Schenck, and H. R. Ott (unpublished).
 - ³⁵ E. Miranda and V. Dobrosavljević, *Physica (Amsterdam) B* **259-261**, 359 (1999).